Magnetic exchange forces and *d*-state filling: Antiferromagnetic MnO(001) and NiO(001) surfaces

M. Granovskij, A. Schrön,[*] and F. Bechstedt

Institut für Festkörpertheorie und -optik, Friedrich-Schiller-Universität, Max-Wien-Platz 1, 07743 Jena, Germany

Magnetic exchange force microscopy (MExFM) is one of the most important methods to investigate the spin structure of magnetic surfaces. However, a deep understanding of the measured spin contrast and the spin-dependent forces is missing. For the prototypical antiferromagnetic MnO(001) and NiO(001) surfaces probed by ferromagnetic Fe tips we demonstrate by means of spin-polarized density functional theory that the differences in the tip-surface interaction are due to the distance-dependent occupation of the transition-metal 3*d* states. While agreement is achieved with recent MExFM measurements of NiO(001), we predict opposite spin-contrast for MnO(001).

I. INTRODUCTION

The fundamental understanding of magnetic and spin-dependent phenomena requires the exploration of spin structures on an atomic scale. Spin-polarized scanning tunneling microscopy provides unprecedented insight into collinear and noncollinear spin structures of magnetic metal films[1] and spin-polarized photoexcited electrons in semiconductors.[2] Even spin friction has been recently observed on the atomic scale.[3] To resolve spin structures on surfaces of insulators, recently the magnetic exchange force microscopy (MExFM) has been developed.[4] Its capability of atomic resolution has been demonstrated for the (001) surface of antiferromagnetic NiO.[5,6] The novel MExFM technique probes variations of the magnitude and relative orientation of surface magnetic moments and not only the chemical contrast.

For the understanding of spin-dependent quantum-mechanical exchange forces between a surface and the tip, the dependence of their strength on the tip-surface distance, and the influence of the atomic geometry, the magnetic exchange interaction has to be separated unambiguously from the chemical interaction. For ferromagnetic samples field-dependent experiments are possible. However, an external magnetic field can change the spin configuration to be explored. In antiferromagnetic samples where chemically identical neighboring atoms carry spins in opposite directions, no external field is needed. Prototypical examples are the (001) cleavage surfaces of transition-metal (TM) oxides MnO, FeO, CoO, and NiO. They are antiferromagnetically ordered below the Néel temperature and crystallize in an only weakly distorted rocksalt structure (see, e.g., Ref. [7]). The TM^{2+} ions mainly carry local magnetic moments which vary with the occupation of the minority-spin t_{2g} states in the localized TM 3*d* shell with 0 (Mn^{2+}), 1 (Fe^{2+}), 2 (Co^{2+}), or 3 (Ni^{2+}) electrons. The TMO(001) cleavage planes remain unreconstructed and exhibit only a slight (5%) rumpling and (2%) relaxation.[8,9] NiO with completely filled t_{2g} shells serves as prototypical TM oxide. Indeed, clean and well defined NiO(001) surfaces can be prepared by *in situ* cleavage. Due to its high Néel temperature of 525 K, NiO exhibits antiferromagnetic ordering at room temperature. First theoretical studies regarding MExFM on this system exist.[10] However, they remain inconclusive, since describing the tip by a single isolated Fe atom results in a unstable tip magnetization versus tip-surface distance.

In this article, we investigate the tip-surface interaction versus distance and surface atoms. To emphasize the influence of the filling of the minority-spin TM 3*d* states we compare MnO(001) and NiO(001). We demonstrate that, despite the chemical and magnetic similarity of the two TMOs, the exchange coupling and the derived spin-dependent forces between the tip and surface atoms vary differently with the distance. We predict a different behavior of the magnetic exchange forces at small distances for MnO(001) and NiO(001). As a consequence opposite magnetic contrast of the TM^{2+} ions is found in the MExFM images. In Sec. II the details of the calculations as well as the modeling of the magnetic surfaces and the probing tip are described. The chemical and magnetic forces between tip and surface as well as the underlying interaction mechanisms are investigated in Sec. III. Finally, we study the consequences for the resulting MExFM images and corrugations in Sec. IV. We conclude the article with a short summary in Sec. V.

II. COMPUTATIONAL DETAILS

Our studies are based on spin-polarized density functional theory (DFT) as implemented in VASP.[11] Exchange and correlation (XC) are described within the local spin density approximation (LDA).[12] The projector-augmented wave (PAW) method is applied to generate pseudopotentials and represent all-electron wave functions in the PAW spheres.[13] In between the PAW spheres a plane-wave expansion up to a cutoff energy of 800 eV is applied. The LDA functional describes better the chemical forces for larger distances, for which van der Waals (vdW) interaction may be important, compared to an XC description including gradient corrections. This has been clearly shown for graphite.[14] To account for the localization of the TM 3*d* electrons, the description of exchange and correlation is improved by an on-site Hubbard repulsion U. We apply the rotationally invariant LDA + U scheme of Anisimov *et al.*[15] with an effective Coulomb parameter $U = 4$ eV for Mn, Fe, and Ni atoms. This value is a reasonable compromise to describe the structural, electronic, and magnetic properties of MnO and NiO and their cleavage faces properly.[7,16,17] Larger U values open the fundamental gap further[18] but give rise to an incorrect energetic ordering of the band symmetries.[16] Also for the Fe atoms in the tip apex the same Coulomb correction is applied.

The TMO(001) surfaces are modeled by symmetric slabs of five atomic layers separated by 23 Å vacuum. The corresponding surface Brillouin zone is sampled by a mesh of $4 \times 4 \times 1$ **k** points. We use a cluster model for the tip.[19] The tip apex is described by a pyramid consisting of five Fe atoms with ferromagnetic ordering. In each lateral magnetic (2×1) surface unit cell we distinguish TM↑ and TM↓ atoms with magnetic moments parallel or antiparallel to the magnetic moments of the ferromagnetic Fe tip. The surface oxygen atoms with TM↑ or TM↓ atoms underneath in the second atomic layer are designated as O↑ and O↓, respectively. The finite lateral extent of the tip apex of 3.4 Å together with the periodic boundary conditions ask for a minimization of the lateral tip-tip interaction. Therefore, we use a $p(2 \times 2)$ periodicity in the force calculations. The chemical forces $F_{\text{chem}}(A\sigma; z)$ in a distance z are calculated for the tip apex above the inequivalent surface atom sites determined by species A = {Mn, Ni, O} and spin orientation $\sigma = \{\uparrow, \downarrow\}$ parallel or antiparallel to the ferromagnetic Fe tip. They are defined as the sum of the Hellmann-Feynman forces acting on the five tip-pyramid atoms. The forces are densely sampled in steps of 0.05 Å for tip-surface distances $1.75 < z < 5$ Å.

III. CHEMICAL AND MAGNETIC FORCES

A. Distance dependence

The resulting chemical forces $F_{\text{chem}}(A\sigma; z)$ acting on the ferromagnetic Fe tip at the lateral positions $A\sigma$ are depicted in Figs. 1(a) and 1(c) in the range $1.8 < z < 3.8$ Å. The exchange forces $F_X(A; z) = F_{\text{chem}}(A\downarrow; z) - F_{\text{chem}}(A\uparrow; z)$ are directly obtained as the differences of the corresponding curves in Figs. 1(a) and 1(c). In Figs. 1(b) and 1(d) the corresponding exchange energies $E_X(A; z) = E(A\downarrow; z) - E(A\uparrow; z)$ are plotted, where $E(A\sigma; z)$ is the total energy of the system for the Fe tip apex at the lateral site $A\sigma$.
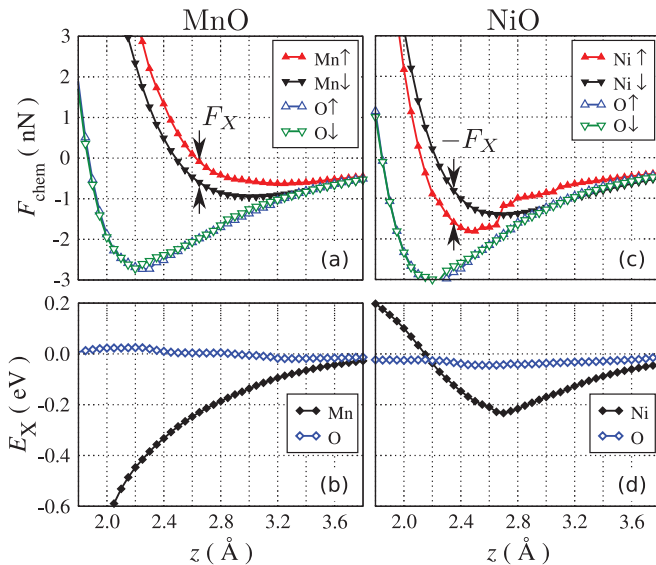

FIG. 1. (Color online) (a), (c) Chemical forces F_{chem} and (b), (d) exchange energies E_X at the lateral positions of the four surface atoms as functions of the tip-surface distance. Left panels (a) and (b) display results for MnO(001), while those for NiO(001) are in the right panels (c) and (d).

The chemical forces show a similar qualitative behavior. They loose their attractive character for large tip-surface distances and indicate a repulsive behavior for small distances. For the tip above the O sites, the minima of $F_{\text{chem}}(O\sigma; z) \approx -3$ nN at $z \approx 2.3$ Å indicate strong attractive interaction between tip and oxygen atoms for both TMOs. The "equilibrium" distance of around 1.9 Å, where $F_{\text{chem}}(O\sigma; z)$ vanishes, is somewhat smaller than the Fe-O bond length in bulk FeO.[7] Above the O sites, the exchange energy E_X almost vanishes. Only for NiO a weak "antiferromagnetic" coupling ($E_X < 0$) is visible, that might be due to superexchange interaction of the Fe tip atoms with the Ni atoms in the second layer mediated by the oxygen atoms in the surface layer.[20,21]

The attraction between TM surface and Fe tip atoms is weaker compared to that between O surface and Fe tip atoms. However, also significant qualitative and quantitative differences between MnO and NiO occur. For MnO, $F_{\text{chem}}(Mn\downarrow; z)$ is below $F_{\text{chem}}(Mn\uparrow; z)$ in the whole range of z; i.e., the tip is attracted more strongly above the Mn↓ site compared to the Mn↑ site. In agreement with the forces, also $E_X(Mn; z)$ indicates a strong antiferromagnetic coupling between Mn and Fe atoms that increases in strength monotonically with decreasing tip-surface distance z. The attractive forces acting on the Fe above the Ni atoms in the NiO surface are stronger compared to the Mn atoms in the MnO surface. Consequently, the minima of $F_{\text{chem}}(Ni\sigma; z)$ are more pronounced and occur at smaller tip-surface distances compared to $F_{\text{chem}}(Mn\sigma; z)$ in MnO. The most important difference is, however, the crossing of $F_{\text{chem}}(Ni\uparrow; z)$ and $F_{\text{chem}}(Ni\downarrow; z)$ near $z = 2.7$ Å that does not occur for MnO. In other words the exchange force $F_X(Ni; z)$ in the NiO case changes from a negative sign at distances $z > 2.7$ Å to a positive one below $z = 2.7$ Å, while $F_X(Mn; z)$ remains negative in the entire range of z. Also in contrast to MnO, the exchange energy $E_X(Ni; z)$ changes its behavior near the critical distance $z = 2.7$ Å, where the antiferromagnetic coupling takes on its maximum with a value of $E_X = -239$ meV. For tip-surface distances below $z = 2.7$ Å, an additional ferromagnetic coupling is found for NiO, that eventually overcomes the antiferromagnetic coupling for $z < 2.2$ Å.

B. Redistribution of spin densities

For the understanding of the different magnetic interactions between the tip and TM surface atoms we analyze the spin-density redistributions $\Delta\rho^\sigma = \rho_{\text{ts}}^\sigma - \rho_{\text{t}}^\sigma - \rho_{\text{s}}^\sigma$ due to the interaction, where ρ_{ts}^σ is the spin-density component σ of the interacting system, and ρ_{t}^σ and ρ_{s}^σ are the spin densities of the noninteracting tip and slab, respectively. In Fig. 2 these spin-density changes are depicted in the (010) plane for the Fe tip positioned above the TM↑ and TM↓ sites. We focus on the tip-surface distance $z = 2.6$ Å just below the crossing point of the $F_{\text{chem}}(Ni\sigma; z)$ curves at $z = 2.7$ Å.

For the Fe tip above the TM↓ surface atoms [Figs. 2(c), 2(d), 2(g), and 2(h)] the behavior is very similar for MnO and NiO. Electrons are transferred from TM states with d_{z^2} character in the majority-spin channel into the minority-spin channel. This holds not only for the TM↓ atoms in the TMO surface, but also for the Fe atom closest to the surface. In the latter case, however, the character of the involved orbitals is not solely d_{z^2} derived but contains also some contributions
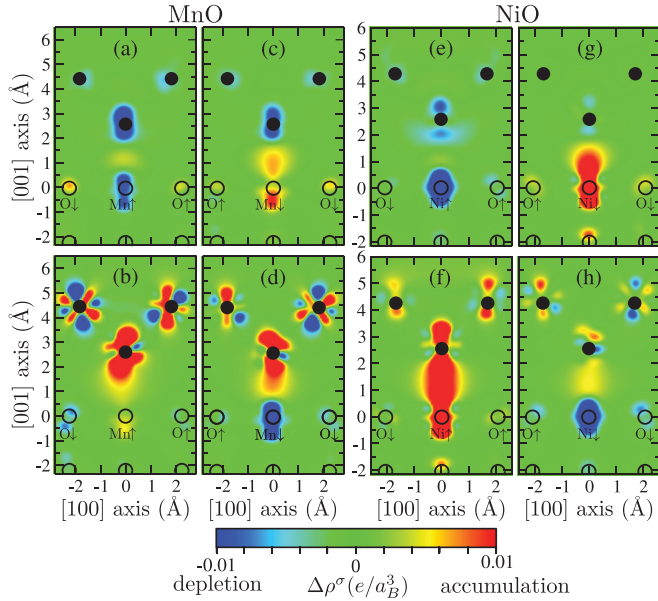
FIG. 2. (Color online) Changes of the spin densities $\Delta\rho^\sigma$ in the (010) plane due to tip-surface interaction for MnO (left panels) and NiO (right panels) at a tip-surface distance $z = 2.6$ Å. The upper (lower) panels display the redistribution of the spin-up density $\Delta\rho^\uparrow$ (spin-down density $\Delta\rho^\downarrow$). Black dots denote Fe↑ tip atoms, while the open circles represent surface atoms in the first two layers. The tip is positioned above the surface TM↑ [(a), (b), (e), and (f)] and TM↓ atoms[(c), (d), (g), and (h)].

of other orbitals. While in NiO [Figs. 2(g) and 2(h)] the redistribution of spin-density is large in the vicinity of the Ni↓ atom and smaller close to the Fe tip atom, the situation is reversed for MnO [Figs. 2(c) and 2(d)].

In contrast to the TM↓ results, striking differences in the spin-density redistributions are found for the Fe tip located above the TM↑ surface atoms [Figs. 2(a), 2(b), 2(e), and 2(f)]. Above the Mn↑ atom [Figs. 2(a) and 2(b)], large redistributions of spin density from the majority- into the minority-spin channel are observed in the vicinity of the Fe tip apex. At the same time, the redistributions of spin density are small in the vicinity of the Mn↑ atom in the MnO surface. For the NiO surface the situation is different [Figs. 2(e) and 2(f)]. Here, large redistributions of spin density occur at both atoms: the Fe tip atom closest to the surface and the Ni↑ atom in the NiO surface. Moreover, a bond between the Fe tip atom and the Ni↑ surface atom is formed in the minority-spin channel in Fig. 2(f).[22] This bond does not occur at tip-surface distances larger than $z = 2.7$ Å. The strong redistribution of spin density into the bonding region below $z = 2.7$ Å causes an additional attractive force between the Fe tip and the Ni↑ atom and, hence, is responsible for the crossing of the $F_{chem}(Ni\sigma;z)$ curves and the sign change of $F_X(Ni;z)$.

C. Interaction mechanisms

The question arises which mechanisms drive the interaction of the Fe tip with the Mn atoms and Ni atoms, respectively. At large tip-surface distances the overlap of the wave functions of the $3d$ electrons located at the Fe tip and the TM atoms in the surface is small. Consequently, the driving interaction

mechanisms are direct Heitler-London exchange[23] in the case of parallel aligned spins, i.e., for the Fe tip located above the TM↑ atom, and indirect kinetic exchange according to Anderson[23] in the case of antiparallel aligned spins, i.e., for the Fe tip located above the TM↓ atom. Kinetic exchange interaction is generally stronger than direct exchange and therefore the antiferromagnetic coupling between Fe tip atoms and surface TM atoms is more favorable at large distances.[23]

At intermediate and small tip-surface distances the picture of weakly overlapping orbitals does not hold anymore. Instead, the formation of spin-dependent molecular orbitals becomes important [see, e.g., Fig. 2(f)]. If the tip is located above the TM↑ surface atom, the bonding orbital derived from the unoccupied minority-spin $3d$ states is shifted toward lower energies with decreasing tip-surface distance. Its occupation depends, however, on the $3d$ state filling of the two TM atoms. The energy splitting between occupied majority-spin and unoccupied minority-spin $3d$ states is smaller for NiO than for MnO due to the empty (filled) minority-spin t_{2g} shell of Mn (Ni).[24] Therefore, the minority-spin bonding orbital between the Ni↑ surface atom and the Fe tip atom is occupied below $z = 2.7$ Å [see Fig. 2(f)], while the one between the Mn↑ surface atom and the Fe tip atom is not. The bond formation is further supported by the lowered energy of the surface state with d_{z^2} character located at the Ni surface atoms.[17] Its energy is almost 1 eV below the energy of the empty bulk e_g states.[17] This mechanism may be related to the "covalent magnetism" described earlier.[22] If the tip is located above the TM↓ atoms, the bonding orbitals in both spin channels are occupied at all tip-surface distances z for both TMOs, due to the antiparallel spin alignment of Fe tip atom and surface TM↓ atom.

IV. MAGNETIC EXCHANGE FORCE IMAGES

In order to show the consequences of different level occupations for experimental MExFM studies, we calculate the normalized frequency shift $\gamma(d)$ including vdW interaction for the minimal tip-surface distance d in the force microscope within the large amplitude approximation.[25,26] The $\gamma(d)$ curves exhibit features qualitatively similar to the behavior of the chemical forces in Fig. 1 for tip-apex positions above the TM↑, TM↓, O↑, and O↓ atoms. They indicate that the chemical forces are solely responsible for the chemical and magnetic contrasts between the surface sites while the vdW forces give rise to some site-independent corrections. For the MExFM images we calculate the corrugation $\Delta d(x,y;\gamma_c) = d(x,y;\gamma_c) - d_{min}(\gamma_c)$, where $d(x,y;\gamma_c)$ is the minimum tip-surface distance at site (x,y) for constant frequency shift γ_c and $d_{min}(\gamma_c)$ is the global minimum tip-surface distance for constant frequency shift γ_c and all sites (x,y). We choose $\gamma_c = -15.5$ fNm$^{1/2}$ for MnO and $\gamma_c = -21.0$ fNm$^{1/2}$ for NiO. The resulting MExFM images and line profiles are displayed in Fig. 3. Pronounced corrugations are visible along the row of four different surface atoms in a magnetic unit cell [Figs. 3(c) and 3(d)]. We find similar spin-averaged chemical contrasts between TM and O sites of 21.4 pm (MnO) and 20.1 pm (NiO) for both TMOs. However, the spin contrast between TM↑ and TM↓ sites is reversed for MnO compared to NiO. It changes from -26.8 pm for MnO to $+11.2$ pm for NiO, i.e., with the different occupation of the minority-spin channel.
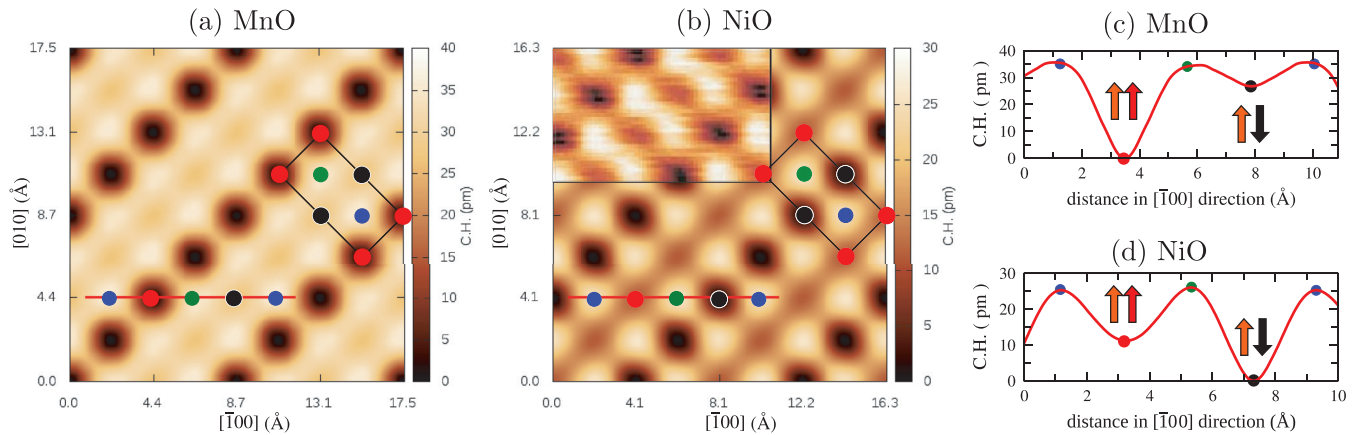
FIG. 3. (Color online) MExFM images of the (a) MnO(001) and (b) NiO(001) surfaces. The inset in (b) shows an experimental MExFM image obtained by Kaiser *et al.* (Ref. [5]). The magnetic 2×1 surface cell with TM↑ (red), TM↓ (black), O↑ (blue), and O↓ (green) atoms is indicated. Line profiles along the [$\bar{1}$00] direction are plotted for (c) MnO and (d) NiO. The corresponding paths on the surfaces are indicated by red lines in (a) and (b), respectively.

For the NiO(001) surface we emphasize the qualitative agreement of the MExFM image in Fig. 3(b) and the line profile in Fig. 3(d) with the measured ones.[5] Quantitatively there are, however, a few differences. The experimental MExFM image has been achieved at a constant frequency shift $\gamma_c = -2.71$ fNm$^{1/2}$ with a chemical contrast of 4.5 pm and a spin contrast of 1.5 pm. It seems that the theoretical model applied here overestimates both the corrugation heights and the frequency shifts. Nevertheless, large corrugations of 40–50 pm have been measured in earlier noncontact AFM studies.[5,27,28] Excluding the empirical vdW corrections,[25] γ_c becomes smaller with values around -5 fNm$^{1/2}$ while at the same time the corrugation increases up to 100 pm.

A treatment of the vdW interaction between tip and surface on a more sophisticated level and the inclusion of the atomic relaxation of tip and surface may improve the predictive power for the distance-dependent forces[19] and the resulting images. The predicted opposite spin-contrasts of NiO(001) and MnO(001) suggest low-temperature MExFM studies also of the MnO(001) surface. The drastic differences in the chemical and magnetic contrast in Fig. 3 with respect to NiO(001) should be detectable and improve our knowledge about the interplay of 3d shell occupation and surface magnetic properties.

V. SUMMARY

We have investigated the chemical and magnetic forces between a ferromagnetic Fe tip and the antiferromagnetically ordered MnO(001) and NiO(001) surfaces for a wide range of tip-surface distances. For MnO, the exchange force between the Fe tip and the Mn surface atoms is negative for all

tip-surface distances. For NiO, the situation is more complex. While for larger tip-surface distances the exchange force is negative, it changes its sign for distances below $z \approx 2.7$ Å.

In order to explain the drastic differences of the exchange forces between an Fe tip and the two chemically and magnetically similar surfaces, we have further investigated the redistribution of the spin densities due to the tip-surface interaction. Below the critical distance $z \approx 2.7$ Å, the formation of a spin-dependent covalent bond occurs between the Fe atom at the tip apex and the Ni surface atoms with the same spin orientation. This leads to an additional attractive force for the ferromagnetic configuration between the Fe tip and Ni surface atoms and, hence, explains the change of the sign of the exchange force.

Finally, we calculated MExFM images and corrugation profiles for both surfaces probed with a ferromagnetic Fe tip. As a consequence of the different sign of the exchange force between the Fe tip and the Mn or Ni surface atoms, the calculated MExFM images show opposite spin contrasts of the TM atoms. We find an outstanding qualitative agreement with the experiments conducted by Kaiser *et al.*[5] for the NiO surface, while the MExFM images calculated for MnO are predictions.

*andreas.schroen@uni-jena.de

[1]R. Wiesendanger, H.-J. Güntherodt, G. Güntherodt, R. J. Gambino, and R. Ruf, Phys. Rev. Lett. **65**, 247 (1990).

[2]K. Sueoka, A. Subagyo, H. Hosoi, and K. Mukasa, Nanotechnology **15**, S691 (2004).

[3]B. Wolter, Y. Yoshida, A. Kubetzka, S.-W. Hla, K. von Bergmann, and R. Wiesendanger, Phys. Rev. Lett. **109**, 116102 (2012).

[4]R. Wiesendanger, Rev. Mod. Phys. **81**, 1495 (2009).

[5]U. Kaiser, A. Schwarz, and R. Wiesendanger, Nature (London) **446**, 522 (2007).

[6]F. Pielmeier and F. J. Giessibl, Phys. Rev. Lett. **110**, 266101 (2013).

[7]A. Schrön, C. Rödl, and F. Bechstedt, Phys. Rev. B **86**, 115134 (2012).

[8]T. Okazawa, Y. Yagi, and Y. Kido, Phys. Rev. B **67**, 195406 (2003).

[9]E. A. Soares, R. Paniago, V. E. de Carvalho, E. L. Lopes, G. J. P. Abreu, and H.-D. Pfannes, Phys. Rev. B **73**, 035419 (2006).

[10]H. Momida and T. Oguchi, Surf. Sci. **590**, 42 (2005).

[11]G. Kresse and J. Furthmüller, Phys. Rev. B **54**, 11169 (1996).

[12]J. P. Perdew and A. Zunger, Phys. Rev. B **23**, 5048 (1981).

[13]G. Kresse and D. Joubert, Phys. Rev. B **59**, 1758 (1999).

[14]F. Ortmann, W. G. Schmidt, and F. Bechstedt, Phys. Rev. Lett. **95**, 186101 (2005).

[15]V. I. Anisimov, J. Zaanen, and O. K. Andersen, Phys. Rev. B **44**, 943 (1991).

[16]C. Rödl, F. Fuchs, J. Furthmüller, and F. Bechstedt, Phys. Rev. B **79**, 235114 (2009).

[17]A. Schrön, M. Granovskij, and F. Bechstedt, J. Phys.: Condens. Matter **25**, 094006 (2013).

[18]M. R. Castell, S. L. Dudarev, G. A. D. Briggs, and A. P. Sutton, Phys. Rev. B **59**, 7342 (1999).

[19]W. A. Hofer, A. J. Fisher, R. A. Wolkow, and P. Grütter, Phys. Rev. Lett. **87**, 236104 (2001).

[20]P. W. Anderson, Phys. Rev. **115**, 2 (1959).

[21]P. W. Anderson, Solid State Phys. **14**, 99 (1963).

[22]A. R. Williams, R. Zeller, V. L. Moruzzi, C. D. Gelatt, Jr., and J. Kübler, J. Appl. Phys. **52**, 2067 (1981).

[23]J. B. Goodenough, Phys. Rev. **120**, 67 (1960).

[24]K. Terakura, T. Oguchi, A. R. Williams, and J. Kübler, Phys. Rev. B **30**, 4734 (1984).

[25]F. J. Giessibl and H. Bielefeldt, Phys. Rev. B **61**, 9968 (2000).

[26]R. García and R. Pérez, Surf. Sci. Rep. **47**, 197 (2002).

[27]M. Schmid, J. Mannhart, and F. J. Giessibl, Phys. Rev. B **77**, 045402 (2008).

[28]H. Hölscher, S. M. Langkat, A. Schwarz, and R. Wiesendanger, Appl. Phys. Lett. **81**, 4428 (2002).